


Research Article

Targeted point mutations of the m⁶A modification in miR675 using RNA-guided base editing induce cell apoptosis

Jindong Hao^{1,*}, Chengshun Li^{1,*}, Chao Lin^{2,*}, Yang Hao^{1,*}, Xianfeng Yu¹, Yidan Xia³, Fei Gao¹, Ziping Jiang³ and  Dongxu Wang¹

¹Laboratory Animal Center, College of Animal Science, Jilin University, Changchun, China; ²Department of Animal Science, Jilin Business and Technology College, Changchun, China; ³Department of Hand Surgery, The First Hospital of Jilin University, Changchun, China

Correspondence: Ziping Jiang (waterjzp@jlu.edu.cn) or Dongxu Wang (wang_dong_xu@jlu.edu.cn)



Methylation of the adenine base at the nitrogen 6 position (m⁶A) is the most common post-transcriptional epigenetic modification of RNA, and it plays a very important role in regulating gene expression. To investigate the role of m⁶A methylation in the expression of non-coding RNA and miRNA, we used a system of adenine base editors (ABEs). Here, we mutated regions up- and downstream of miRNA 675 m⁶A modification sites in the *H19* locus using HEK293T, L02, MHCC97L, MHCC97H, A549, and SGC-7901 cells. Our results showed that a T–A base transversion had occurred in all cell lines. Moreover, mutation of the regions upstream of the miRNA 675 m⁶A modification site led to reduced expression of *H19* and the induction of cell apoptosis in HEK293T cells. To further confirm our results, L02 and MHCC97L cells were detected using ABEs system. The results indicated increased cell apoptosis and reduced expression of miR675 as well as *H19*. To confirm the relationship between *H19* and miR675 expression, overexpression and knockdown studies were performed. The results showed that reduced *H19* expression induced cell apoptosis through miR675. Taken together, these results indicate that m⁶A modification can regulate the expression of *H19* and miR675 which induce cell apoptosis.

Introduction

The long noncoding RNA (lncRNA) *H19* plays a crucial role in the development of cancer [1]. miR675, derived from exon 1 of *H19*, has been shown to have an oncogenic role in liver cancers [2,3]. Our previous data suggest that reduced expression of *H19* could induce cell apoptosis in A549, a lung cancer cell line [4]. Moreover, previous studies have shown that the *H19*/miR675 axis can regulate cell apoptosis [5]. These results demonstrate that altered expression of *H19* or miR675 can influence tumor cell behavior.

Recent reports have suggested that m⁶A (methylation of the adenine base at the nitrogen 6 position) methylation plays an important role in the post-transcriptional modification of RNA [6], and it is known that this modification is regulated by adenosine methyltransferases and demethylases [7,8]. As ‘writers,’ the m⁶A methyltransferases *METTL3*, *METTL14*, and *WTAP* methylate the N6 position of adenosine [9,10]. As ‘erasers,’ the m⁶A demethylases *FTO* and *ALKBH5* reverse the RNA methylation process [11,12]. Finally, *YTHDF2*, as an m⁶A ‘reader,’ recognizes m⁶A sites on target mRNAs and regulates the mRNAs’ fate [13–15]. Indeed, there is evidence that m⁶A modification in microRNA and lncRNA affects cell development and fate [16]. These data indicate that m⁶A modification might have a role in noncoding RNA as well as miRNA.

Currently, the CRISPR/Cas9 system is the most widely used gene-editing tool. It uses an RNA-guide Cas9 protein combined with a short RNA (sgRNA) to induce double-strand breaks in target genomic

*These authors contributed equally to this work.

Received: 20 August 2019

Revised: 09 April 2020

Accepted: 22 April 2020

Accepted Manuscript online:
23 April 2020

Version of Record published:
05 May 2020

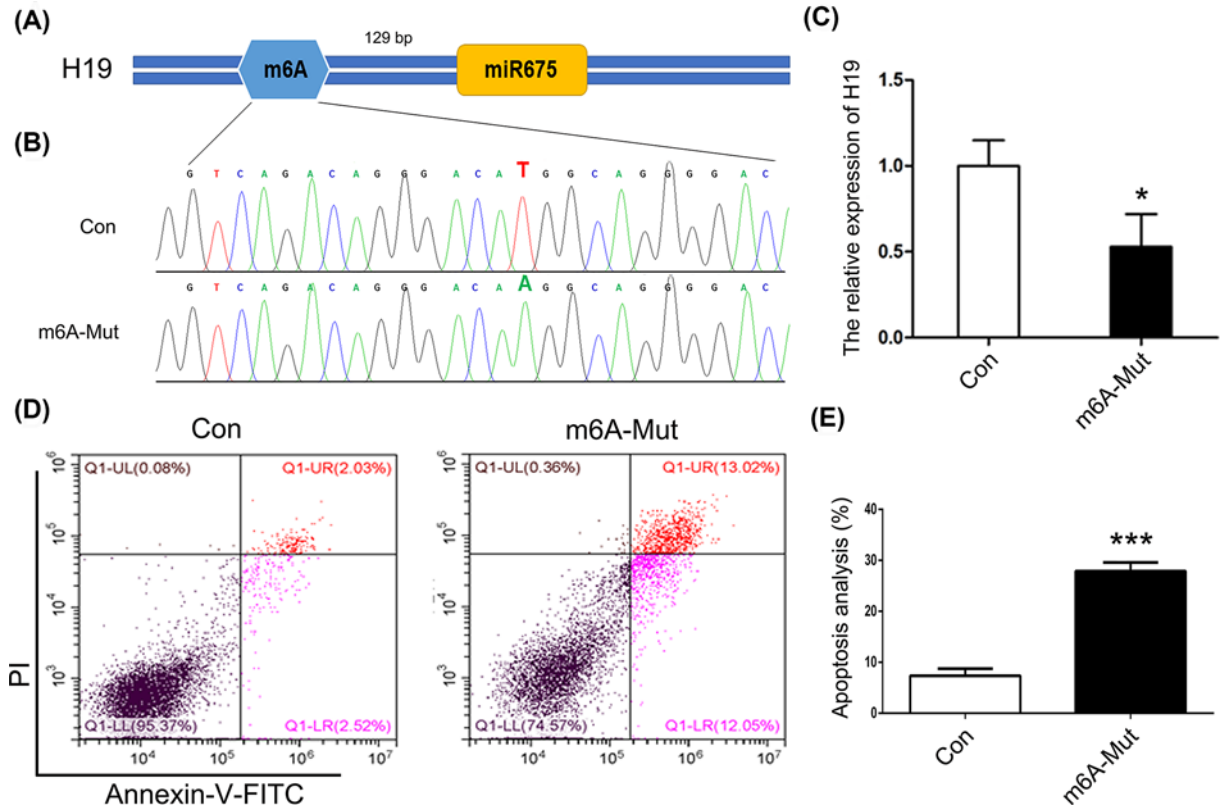


Figure 1. The role of m⁶A modification upstream of miR675

(A) The schematic of m⁶A modification. (B) Sequencing analysis of the m⁶A modification site. (C) *H19* expression analyzed by qPCR. (D) Cell apoptosis was analyzed after mutation of the m⁶A modification site. (E) Statistical analysis of apoptotic cell percentage. The data are presented as the mean \pm SD. * ($P < 0.05$) and *** ($P < 0.005$) indicate statistically significant differences.

DNA [17]. The adenine base editors (ABEs) system, which is based on the CRISPR/Cas9 platform, efficiently converts targeted A•T base pairs into G•C [18]. In the present study, the ABE7.10 system was used to analyze m⁶A modification of miRNA 675 in the *H19* locus. Moreover, cell apoptosis and m⁶A expression levels were evaluated in HEK293T, L02, and MHCC97L cells. The role of m⁶A modification in the expression patterns of miRNA and lncRNA was analyzed using the ABEs system.

Materials and methods

Cell culture

HEK293T, L02, MHCC97L, MHCC97H, SGC-7901, and A549 cells were cultured in Dulbecco's modified Eagle's medium, high glucose (Gibco, U.S.A.), supplemented with 10% fetal bovine serum (Gibco, U.S.A.). The cells were maintained at 37°C in 5% CO₂.

Construction and transfection of the plasmids

ABE7.10 plasmids were obtained from Addgene (102919). The m⁶A modification of miR675 in the *H19* locus (upstream of position: chr11:2018320 and downstream of position: chr11:2017630) was analyzed using the online software tool m6AVar (<http://m6avar.renlab.org>).

Protocols for sgRNA design and the procedures required for *in vitro* transcription have been described previously [17]. The sgRNA-oligo sequences used in the present study are listed in Supplementary Table S1.

For cell transfection, HEK293T, L02, MHCC97L, MHCC97H, SGC-7901, and A549 cells were seeded into 48-well poly-D-lysine-coated plates (Corning) in the absence of any antibiotic. Twelve to fifteen hours after plating, cells were transfected with 750 ng of base-editor plasmid and 250 ng of guide RNA plasmid in the presence of 1 μ l of Lipofectamine 2000 (Thermo Fisher Scientific).

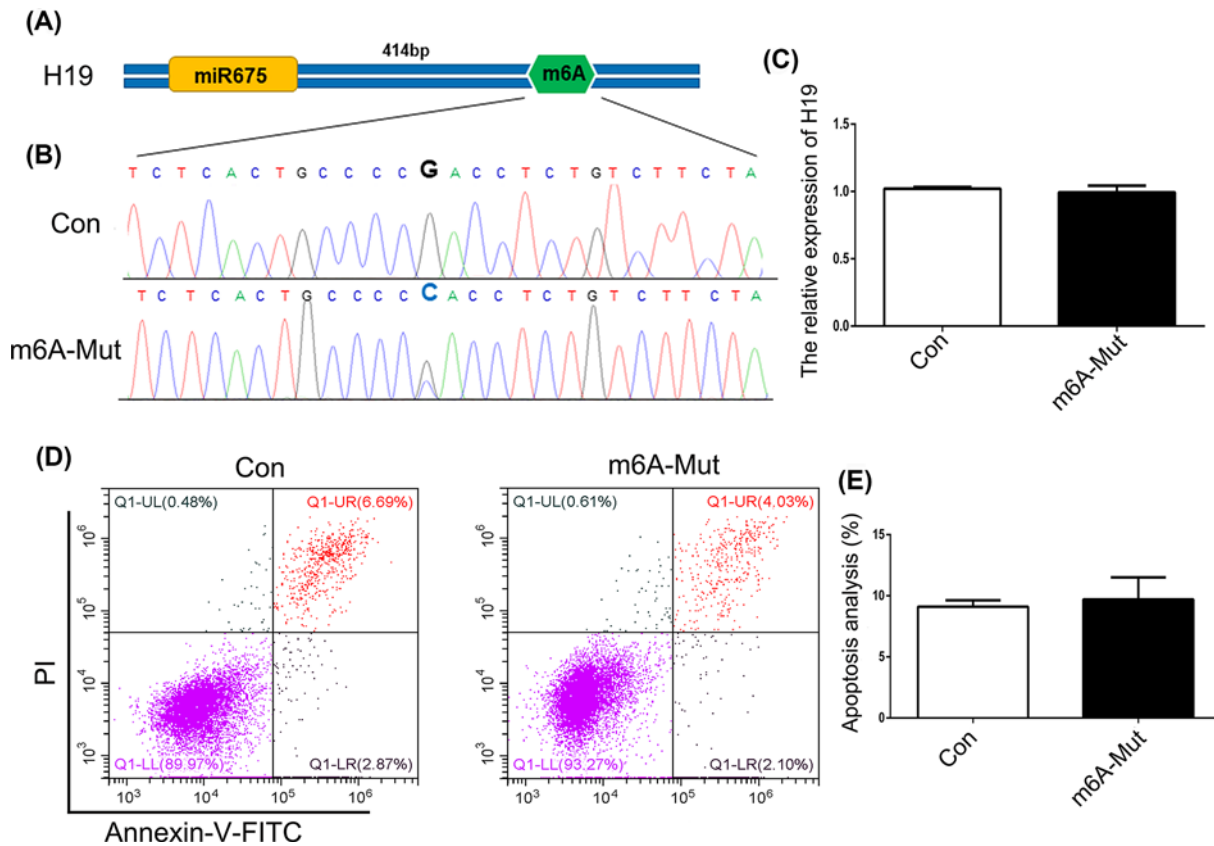


Figure 2. The role of m⁶A modification downstream of miR675

(A) The schematic of m⁶A modification. (B) Sequencing analysis of the m⁶A modification site. (C) H19 expression was analyzed by qPCR. (D) Cell apoptosis was analyzed after mutation of the m⁶A modification site. (E) Statistical analysis of apoptotic cell percentage. The data are presented as the mean ± SD.

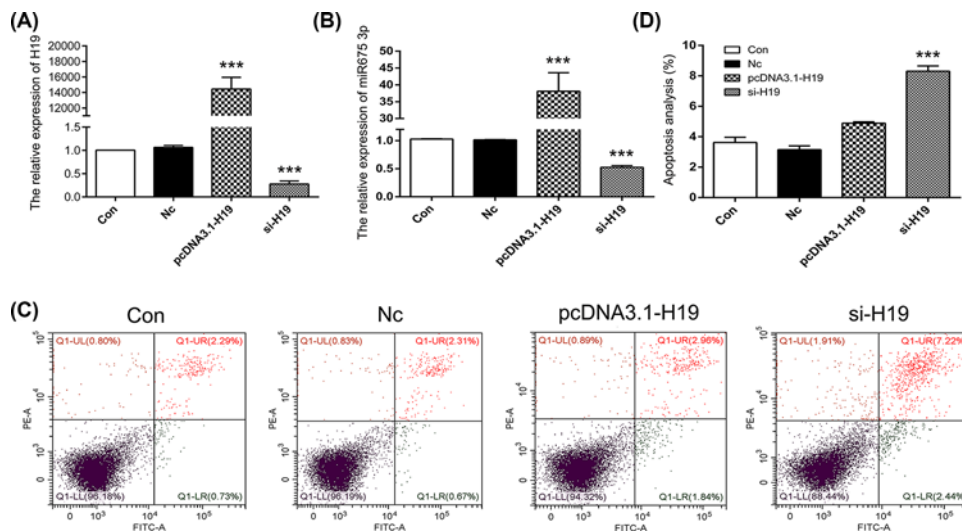


Figure 3. The expression pattern of H19 in apoptosis

Expression of H19 (A) and miR675-3p (B) were analyzed by qPCR. (C) Cell apoptosis was analyzed after mutation of the m⁶A modification site. (D) Statistical analysis of apoptotic cell percentage. The data are presented as the mean ± SD. *** ($P < 0.005$) indicates a statistically significant difference.

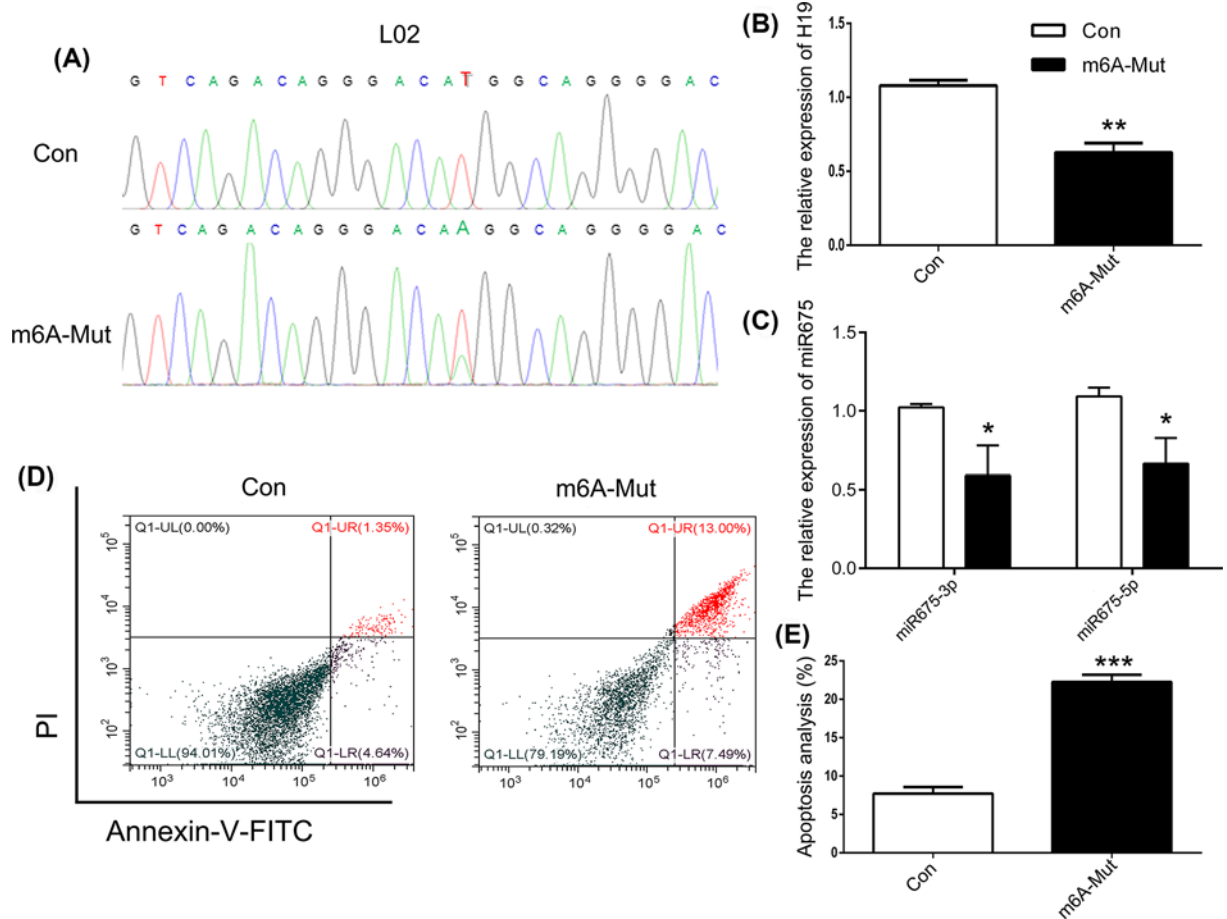


Figure 4. Mutated m⁶A modification of miR675 expression in L02 cells
 (A) Sequencing analysis of m⁶A modification site. The expression of *H19* (B) and miR675 (C) were analyzed by qPCR. (D) Cell apoptosis was analyzed after mutation of the m⁶A modification site. (E) Statistical analysis of apoptotic cell percentage. The data are presented as the mean \pm SD. * ($P < 0.05$), ** ($P < 0.01$) and *** ($P < 0.005$) indicate statistically significant differences.

Knockdown and overexpression of *H19* and miR675

Synthetic RNA oligonucleotides targeting *H19* were obtained from RiboBio (Guangzhou, China). The siRNA target sequence was GCGGGTCTGTTTCTTACT. pcDNA3.1-*H19* was purchased from GenePharma (Shanghai, China). miR675-3p-mimics and miR675-3p-inhibitor were obtained from RiboBio (Guangzhou, China). HEK293T cells were transfected with si-*H19*, pcDNA3.1-*H19*, miR675-3p-mimics, and miR675-3p-inhibitor for 48 h, respectively. Control cells were transfected with nonspecific, scrambled siRNA.

Gene expression analysis

Total RNA was extracted from cells using the AllPrep DNA/RNA Micro Kit (QIAGEN, Germany) according to the manufacturer's instructions. cDNA was synthesized using the First-Strand cDNA Synthesis kit (Promega, U.S.A.). Quantitative real-time PCR (qRT-PCR) was performed to determine *H19*, miR675, and m⁶A-related gene expression using the BioEasy SYBR Green I Real-Time PCR Kit on Bio-Rad iQ5 Multicolor Real-Time PCR Detection System (Bioer Technology, China). The miR675 3p and 5p sequences are listed in Supplementary Table S2, and the miRNA primer sequences are listed in Supplementary Table S3. The primer sequences of m⁶A-related genes and *H19* are listed in Supplementary Table S4. For PCR, the initial denaturation was conducted at 95°C for 3 min, followed by 40 cycles of denaturation at 95°C for 10 s, annealing at 60°C for 15 s, and extension at 72°C for 30 s. The $2^{-\Delta\Delta C_T}$ method was used to determine relative gene expression. The experiments were performed at least in triplicates.

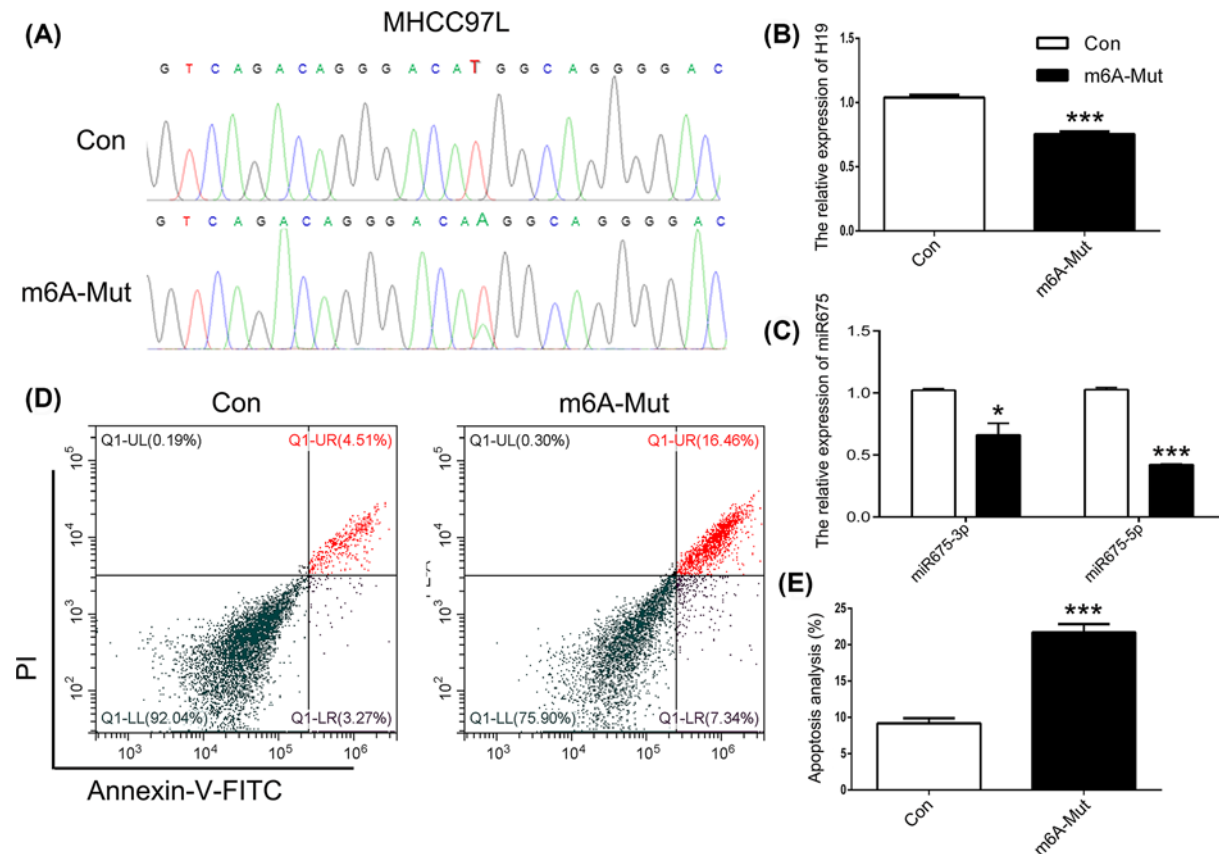


Figure 5. Mutated m⁶A modification of miR675 in MHCC97L cells

(A) Sequencing analysis of the m⁶A modification site. The expression of H19 (B) and miR675 (C) were analyzed by qPCR. (D) Cell apoptosis was analyzed after mutation of the m⁶A modification site. (E) Statistical analysis of apoptotic cell percentage. The data are presented as the mean ± SD. * ($P < 0.05$) and *** ($P < 0.005$) indicate statistically significant differences.

Cell apoptosis analysis

The procedure for cell apoptosis detection has been previously described [19]. Briefly, HEK293T, L02, and MHCC97L cells were used for Annexin V-FITC/PI staining after treatment with ABE7.10 plasmids, si-H19, pcDNA3.1-H19 and miR675-3p-mimics and inhibitor for 48 h. Following incubation, the cells were washed twice with PBS and pooled at a concentration of 1×10^6 cells/ml. For each treated cell sample, Annexin V-FITC and PI were added according to the manufacturer's instructions. These cells were incubated for 30 min and then analyzed with an Accuri™ C6 flow cytometer (BD Biosciences, Franklin Lakes, NJ, U.S.A.).

Immunofluorescence staining

Briefly, the cells were washed three times in PBS and then fixed with 4% paraformaldehyde for 30 min at room temperature. After fixation, the cells were washed again with PBS containing 0.2% Triton X-100 for 30 min. The cells were then incubated in PBS containing 1% bovine serum albumin (BSA) for 1 h. Next, the cells were probed with m⁶A (1:500, Abcam) antibodies and incubated at 4°C overnight. Following this, the cells were washed three times with PBS for 10 min each followed by incubation with Alexa Fluor 488-conjugated secondary (anti-rabbit) antibodies for 1 h at room temperature. DNA was stained with 10 ng/ml Hoechst 33342 (Thermo Scientific) for 15–20 min. The cells were then washed thrice with PBS for 10 min each, air-dried, and mounted on a coverslip and a glass slide using an antifade mounting medium (BOSTER, China). A confocal laser scanning microscope was used for imaging.

Statistical analysis

All data were analyzed using GraphPad Prism 5.0 (GraphPad Software, Inc., San Diego, CA). A *t* test (Unpaired *t* test) was used to analyze the data. A *P*-value < 0.05 was considered statistically significant.

Results

Targeted point mutations of m⁶A modification sites induce cell apoptosis

To investigate the role of m⁶A modification in the expression of *H19*, the ABE7.10 system was used. The m⁶A modification site 129 bp upstream of miR675 in the *H19* locus was mutated in HEK293T cells (Figure 1A). Results of Sanger sequencing suggested T–A base transversion (Figure 1B). To confirm these results, similar tests were carried out with MHCC97H, SGC-7901, and A549 cells. The results confirmed T–A base transversion (Supplementary Figure S1). qPCR results showed decreased expression of *H19* in the m⁶A-Mut group compared with that in the Con group (Figure 1C). To decipher the biological impact of m⁶A modification, we examined cell apoptosis. Our results indicated an increased apoptosis rate in the m⁶A-Mut group (Figure 1D,E). To further confirm the importance of m⁶A modification to *H19* as well as to miR675, we mutated the m⁶A modification site 414 bp downstream of miR675 (Figure 2A). Results of Sanger sequencing suggested G–C base transversion (Figure 2B). qPCR results showed no difference in *H19* expression between the Con and m⁶A-mut groups (Figure 2C). Moreover, the cell apoptosis rate did not increase after point mutations of the m⁶A modification sites (Figure 2D,E). To further analyze *H19* expression patterns in apoptotic cells, knockdown or overexpression of *H19* was performed in HEK293T cells. The results showed that *H19* expression was reduced after transfection with si-*H19* and was increased following transfection with pcDNA3.1-*H19* (Figure 3A). miR675-3p expression was analyzed by qPCR. The results showed that the miR675-3p expression was similar to the expression pattern of *H19* (Figure 3B). The cell apoptosis results showed that reduced expression of *H19* induced cell death (Figure 3C,D). These results indicate that m⁶A modification regulates *H19* expression which may induce cell apoptosis.

Targeted point mutations of m⁶A modification sites in liver cancer cells

To further confirm that point mutations of m⁶A modification sites 129 bp upstream of miR675 induce cell apoptosis, we used L02 and MHCC97L cells. Results of Sanger sequencing showed identical point mutation patterns in both HEK293T and L02 cells (Figure 4A). qPCR results showed declined *H19* expression in the m⁶A-Mut group (Figure 4B). To investigate the effects of m⁶A modification on the expression patterns of miRNA, the expression of miR675 was analyzed. The results showed decreased expression of both miR675-3p and miR675-5p (Figure 4C). In addition, an increased cell apoptosis rate was observed in the m⁶A-Mut group (Figure 4D,E). To confirm that point mutations do induce cell apoptosis, the MHCC97L cell line (liver cancer cells) was used. As observed with HEK293T and L02 cells, a T–A base transversion was observed in MHCC97L cells (Figure 5A). Moreover, decreased expression of *H19*, miR675-3p, and miR675-5p was noted in MHCC97L cells in the m⁶A-Mut group (Figure 5B,C). An increased cell apoptosis rate was observed in MHCC97L cells after the introduction of point mutations as observed in HEK293T and L02 cells (Figure 5D,E). To further analyze miR675 expression patterns in apoptotic cells, HEK293T cells were treated with a mimic or inhibitor of miR675-3p. The results showed that reduced miR675-3p expression induced cell apoptosis (Figure 6). These results suggest that targeted point mutations of m⁶A modification sites 129 bp upstream of miR675 induced cell apoptosis through reduced expression of *H19*.

m⁶A-related genes expression analysis by targeted point mutation

We further explored the expression patterns of m⁶A-related genes after introducing point mutations in L02 and MHCC97L cells. qPCR results showed increased expression of *ALKBH5* and decreased expression of *METTL3*, *METTL14*, *WTAP*, *FTO*, and *YTHDF2* in MHCC97L cells compared with L02 cells (Figure 7A). This result suggested that compared with L02, there is abnormal expression of m⁶A genes in MHCC97L cells. However, the expression of m⁶A-related genes was not changed by point mutations in L02 and MHCC97L cells (Figure 7B,C). m⁶A expression level was analyzed using immunofluorescence (IF). The results showed that m⁶A expression was not altered in either L02 and MHCC97L cells (Figure 7D,E). Also, the statistical analysis confirmed the IF data (Figure 7F,G). These results indicated that targeted point mutations of miR675 did not change the global m⁶A expression levels in L02 and MHCC97L cells.

Discussion

Previous reports have indicated that targeted point mutations result in C-to-T (BE3) or A-to-G (ABE7.10) conversions [18,20]. In this study, our results showed that a T–A base transversion occurred upstream of miR675 in HEK293T, L02, and MHCC97L cells. While the expected result was an A•T to G•C conversion, our data showed that an A•T to A•A conversion had occurred. These results indicate the partial effectiveness of the ABE7.10 system, which might have induced cell apoptosis. To confirm these data, we transfected the ABE7.10 system into A549 (lung cancer cells),

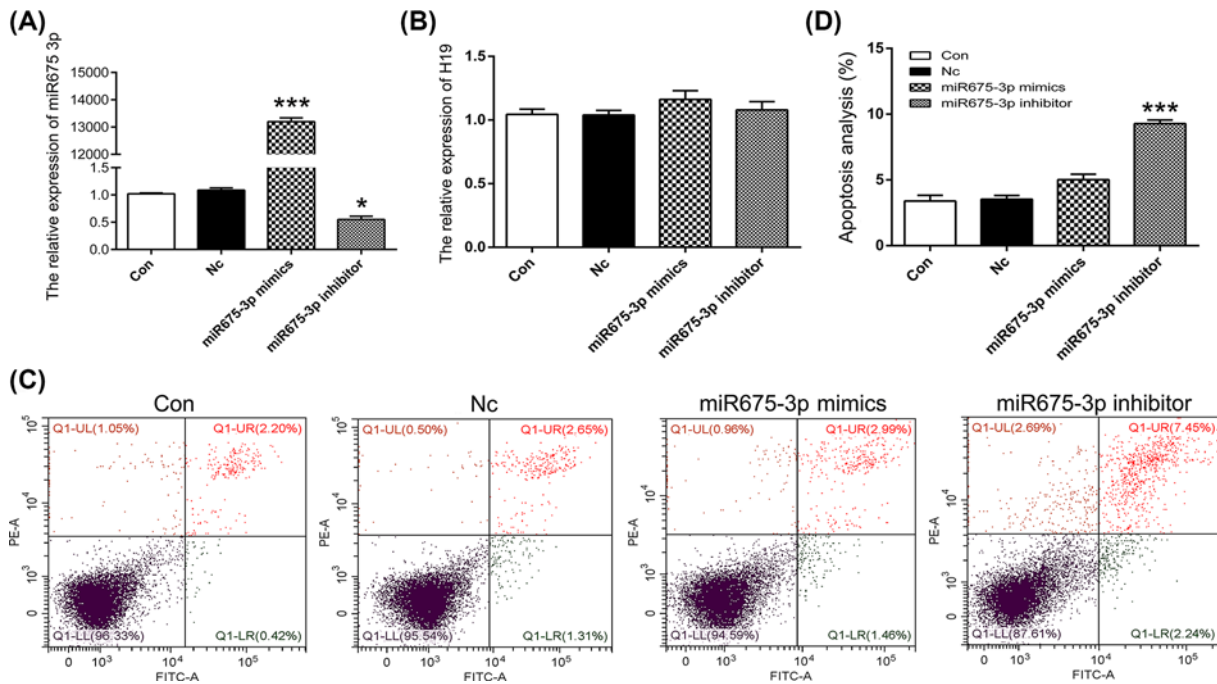


Figure 6. The expression pattern of miR675-3p in apoptosis

The expression of miR675-3p (A) and *H19* (B) were analyzed by qPCR. (C) Apoptosis was analyzed after mutation of the m⁶A modification site. (D) Statistical analysis of apoptotic cell percentage. The data are presented as the mean \pm SD. * ($P < 0.05$) and *** ($P < 0.005$) indicate statistically significant differences.

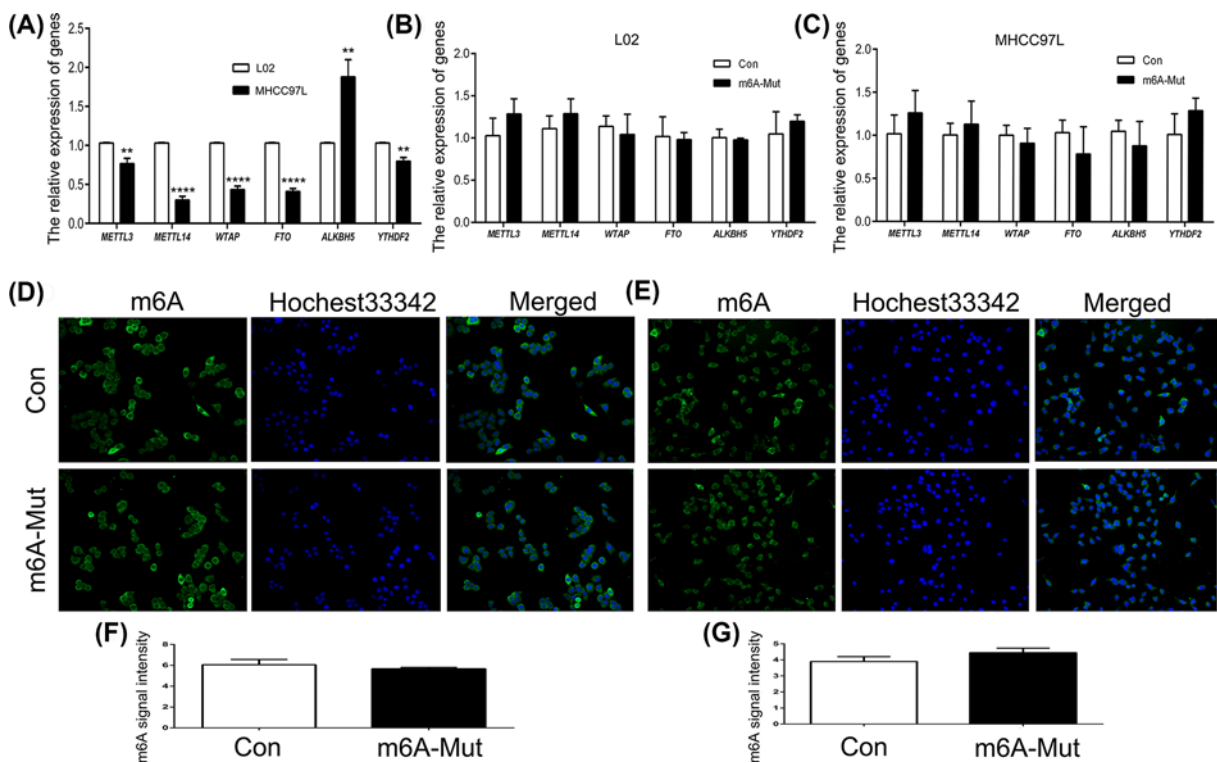


Figure 7. Expression pattern of m⁶A-related genes

The expression of m⁶A-related genes was analyzed in L02 and MHCC97L cells (A). The expression of m⁶A-related genes analyzed by point mutations in L02 (B) and MHCC97L (C) cells. IF localization of m⁶A in L02 (D) and MHCC97L (E) cells. The fluorescence intensities of m⁶A were measured in L02 (F) and MHCC97L (G) cells. ** ($P < 0.01$) and **** ($P < 0.001$) indicate statistically significant differences.

SGC7901 (gastric cancer cells), and MHCC97H (liver cancer cells) cells. The result was in accordance with our previous data. In addition, a G-to-A conversion was observed which might have indicated incomplete mutation downstream of miR675. These results suggested the presence of the T–A base conversion pattern, which might have a role in cell apoptosis.

To further investigate the role of m⁶A modification in apoptosis, the expression patterns of *H19* and miR675 were analyzed. A previous study suggested that m⁶A modification was important for the expression of lncRNA and miRNA [21]. In our study, regions upstream and downstream of the m⁶A modification site of miR675 in the *H19* locus were evaluated. The results demonstrated that mutations in the regions upstream of the m⁶A modification site could suppress the expression of *H19* and miR675, whereas mutations in the regions downstream of the m⁶A modification site have no effect on the expression of *H19* and miR675. To confirm the expression patterns of *H19* and miR675 in apoptotic cells, overexpression and knockdown of *H19* and miR675 were examined. Previous reports showed that the expression of *H19* and miR675 was associated with cell apoptosis in cancer cells [22,23]. Our data suggest that reduced *H19* expression induced cell apoptosis through miR675, which was confirmed in human colorectal cancer cells [24]. These results indicate that regions upstream of the m⁶A modification site play a role in regulating the expression of *H19* and miR675 which can induce cell apoptosis.

There is evidence that reduced *H19* and miR675 expression led to increased p53 protein expression, which regulates cell apoptosis [25]. Our data showed that mutation of the regions upstream of the m⁶A modification site inhibited miR675 and *H19* expression, inducing cell apoptosis, possibly through the p53 protein. Moreover, an abnormal expression pattern of m⁶A-related genes was observed in liver cancer cells, which was in accordance with previous data [26]. A previous report suggested that *ALKBH5* overexpression promotes invasion and metastasis in gastric cancer cells [27]. Indeed, metastasis is the major factor for HCC. This indicates that *ALKBH5* expression may regulate the demethylated process and play a role in HCC metastasis. In addition, the global m⁶A expression was maintained after mutations of the regions upstream of the m⁶A modification site in L02 and MHCC97L cells. These results suggested that miR675 was regulated by m⁶A modification and has a role in *H19* expression, which in turn influences the fate of the cell.

Conclusion

In summary, the ABE7.10 system resulted in efficient T–A base conversion of the m⁶A site upstream of miR675 in the *H19* locus. The expression of *H19* and miR675 was reduced by targeted point mutations. These mutations also induced cell apoptosis. Overall, our data suggest that m⁶A modification plays a role in gene expression and cell apoptosis.

Competing Interests

The authors declare that there are no competing interests associated with the manuscript.

Funding

This work was supported by the National Natural Science Foundation of China [grant number 31601003]; the China Postdoctoral Science Foundation [grant numbers 018T110250, 2016M601384]; the Fundamental Research Funds for the Central Universities [grant number 2019JCKT-70]; the Natural Science Foundation [grant number 2018SCZWSZX-045]; the Jilin Education Department Program [grant number JJKH20200950KJ]; and the Jilin Scientific and Technological Development Program [grant numbers 20190103071JH, 20180101254JC, 20170623093-TC].

Author Contribution

Dongxu Wang designed the experiments and wrote the manuscript. Jindong Hao, Chengshun Li, Yang Hao and Yidan Xia performed cell experiment and gene expression analysis. Xianfeng Yu and Ziping Jiang contributed reagents and materials. Fei Gao and Chao Lin analyzed the data and prepared figures. All authors reviewed the manuscript.

Abbreviations

ABE, adenine base editor; IF, immunofluorescence; lncRNA, long noncoding RNA; m⁶A, methylation of the adenine base at the nitrogen 6 position; PI, Propidium Iodide; qPCR, Quantitative Real-time PCR.

References

- Schwarzenbach, H. (2016) Biological and clinical relevance of H19 in colorectal cancer patients. *EBioMedicine* **13**, 9–10, <https://doi.org/10.1016/j.ebiom.2016.11.001>

- 2 Hao, Y., Crenshaw, T., Moulton, T., Newcomb, E. and Tycko, B. (1993) Tumour-suppressor activity of H19 RNA. *Nature* **365**, 764–767, <https://doi.org/10.1038/365764a0>
- 3 Li, H., Li, J., Jia, S., Wu, M., An, J., Zheng, Q. et al. (2015) miR675 upregulates long noncoding RNA H19 through activating EGR1 in human liver cancer. *Oncotarget* **6**, 31958–31984
- 4 Hao, Y., Wang, G., Lin, C., Li, D., Ji, Z., Gao, F. et al. (2017) Valproic acid induces decreased expression of H19 promoting cell apoptosis in A549 cells. *DNA Cell Biol.* **36**, 428–435, <https://doi.org/10.1089/dna.2016.3542>
- 5 Li, X., Wang, H., Yao, B., Xu, W., Chen, J. and Zhou, X. (2016) lncRNA H19/miR-675 axis regulates cardiomyocyte apoptosis by targeting VDAC1 in diabetic cardiomyopathy. *Sci. Rep.* **6**, 36340, <https://doi.org/10.1038/srep36340>
- 6 Zhao, B.S., Wang, X., Beadell, A.V., Lu, Z., Shi, H., Kuuspalu, A. et al. (2017) m(6)A-dependent maternal mRNA clearance facilitates zebrafish maternal-to-zygotic transition. *Nature* **542**, 475–478, <https://doi.org/10.1038/nature21355>
- 7 Geula, S., Moshitch-Moshkovitz, S., Dominissini, D., Mansour, A.A., Kol, N., Salmon-Divon, M. et al. (2015) Stem cells. m6A mRNA methylation facilitates resolution of naive pluripotency toward differentiation. *Science* **347**, 1002–1006, <https://doi.org/10.1126/science.1261417>
- 8 Dominissini, D., Moshitch-Moshkovitz, S., Schwartz, S., Salmon-Divon, M., Ungar, L., Osenberg, S. et al. (2012) Topology of the human and mouse m6A RNA methylomes revealed by m6A-seq. *Nature* **485**, 201–206, <https://doi.org/10.1038/nature11112>
- 9 Ping, X.L., Sun, B.F., Wang, L., Xiao, W., Yang, X., Wang, W.J. et al. (2014) Mammalian WTAP is a regulatory subunit of the RNA N6-methyladenosine methyltransferase. *Cell Res.* **24**, 177–189, <https://doi.org/10.1038/cr.2014.3>
- 10 Li, H.B., Tong, J., Zhu, S., Batista, P.J., Duffy, E.E., Zhao, J. et al. (2017) m(6)A mRNA methylation controls T cell homeostasis by targeting the IL-7/STAT5/SOCS pathways. *Nature* **548**, 338–342, <https://doi.org/10.1038/nature23450>
- 11 Feng, C., Liu, Y., Wang, G., Deng, Z., Zhang, Q., Wu, W. et al. (2014) Crystal structures of the human RNA demethylase Alkbh5 reveal basis for substrate recognition. *J. Biol. Chem.* **289**, 11571–11583, <https://doi.org/10.1074/jbc.M113.546168>
- 12 Zheng, Q., Hou, J., Zhou, Y., Li, Z. and Cao, X. (2017) The RNA helicase DDX46 inhibits innate immunity by entrapping m(6)A-demethylated antiviral transcripts in the nucleus. *Nat. Immunol.* **18**, 1094–1103, <https://doi.org/10.1038/ni.3830>
- 13 Nguyen, L.H., Robinton, D.A., Seligson, M.T., Wu, L.W., Li, L., Rakheja, D. et al. (2014) Lin28b is sufficient to drive liver cancer and necessary for its maintenance in murine models. *Cancer Cell* **26**, 248–261, <https://doi.org/10.1016/j.ccr.2014.06.018>
- 14 Huang, H., Weng, H., Sun, W., Qin, X., Shi, H., Wu, H. et al. (2018) Recognition of RNA N(6)-methyladenosine by IGF2BP proteins enhances mRNA stability and translation. *Nat. Cell Biol.* **20**, 285–295, <https://doi.org/10.1038/s41556-018-0045-z>
- 15 Wang, X. and He, C. (2014) Reading RNA methylation codes through methyl-specific binding proteins. *RNA Biol.* **11**, 669–672, <https://doi.org/10.4161/rna.28829>
- 16 Fazi, F. and Fatica, A. (2019) Interplay between N-6-Methyladenosine (m(6)A) and non-coding RNAs in cell development and cancer. *Front. Cell Dev. Biol.* **7**, <https://doi.org/10.3389/fcell.2019.00116>
- 17 Cong, L., Ran, F.A., Cox, D., Lin, S., Barretto, R., Habib, N. et al. (2013) Multiplex genome engineering using CRISPR/Cas systems. *Science* **339**, 819–823, <https://doi.org/10.1126/science.1231143>
- 18 Gaudelli, N.M., Komor, A.C., Rees, H.A., Packer, M.S., Badran, A.H., Bryson, D.I. et al. (2017) Programmable base editing of A*T to G*C in genomic DNA without DNA cleavage. *Nature* **551**, 464–471, <https://doi.org/10.1038/nature24644>
- 19 William-Faloutsos, S., Rouillard, D., Lechat, P. and Bastian, G. (2006) Cell cycle arrest and apoptosis induced by oxaliplatin (L-OHP) on four human cancer cell lines. *Anticancer Res.* **26**, 2093–2099
- 20 Komor, A.C., Kim, Y.B., Packer, M.S., Zuris, J.A. and Liu, D.R. (2016) Programmable editing of a target base in genomic DNA without double-stranded DNA cleavage. *Nature* **533**, 420–424, <https://doi.org/10.1038/nature17946>
- 21 Coker, H., Wei, G. and Brockdorff, N. (2019) m6A modification of non-coding RNA and the control of mammalian gene expression. *Biochim. Biophys. Acta Gene Regul. Mech.* **1862**, 310–318, <https://doi.org/10.1016/j.bbagrm.2018.12.002>
- 22 Zhu, M., Chen, Q., Liu, X., Sun, Q., Zhao, X., Deng, R. et al. (2014) lncRNA H19/miR-675 axis represses prostate cancer metastasis by targeting TGFBI. *FEBS J.* **281**, 3766–3775, <https://doi.org/10.1111/febs.12902>
- 23 Zhuang, M., Gao, W., Xu, J., Wang, P. and Shu, Y. (2014) The long non-coding RNA H19-derived miR-675 modulates human gastric cancer cell proliferation by targeting tumor suppressor RUNX1. *Biochem. Biophys. Res. Commun.* **448**, 315–322, <https://doi.org/10.1016/j.bbrc.2013.12.126>
- 24 Tsang, W.P., Ng, E.K., Ng, S.S., Jin, H., Yu, J., Sung, J.J. et al. (2010) Oncofetal H19-derived miR-675 regulates tumor suppressor RB in human colorectal cancer. *Carcinogenesis* **31**, 350–358, <https://doi.org/10.1093/carcin/bgp181>
- 25 Zheng, Z.H., Wu, D.M., Fan, S.H., Zhang, Z.F., Chen, G.Q. and Lu, J. (2019) Upregulation of miR-675-5p induced by lncRNA H19 was associated with tumor progression and development by targeting tumor suppressor p53 in non-small cell lung cancer. *J. Cell. Biochem.* **120**, 18724–18735, <https://doi.org/10.1002/jcb.29182>
- 26 Ma, J.Z., Yang, F., Zhou, C.C., Liu, F., Yuan, J.H., Wang, F. et al. (2017) METTL14 suppresses the metastatic potential of hepatocellular carcinoma by modulating N(6)-methyladenosine-dependent primary microRNA processing. *Hepatology* **65**, 529–543, <https://doi.org/10.1002/hep.28885>
- 27 Zhang, J., Guo, S., Piao, H.Y., Wang, Y., Wu, Y., Meng, X.Y. et al. (2019) ALKBH5 promotes invasion and metastasis of gastric cancer by decreasing methylation of the lncRNA NEAT1. *J. Physiol. Biochem.* **75**, 379–389, <https://doi.org/10.1007/s13105-019-00690-8>